

Impact of Sensing Coverage on Greedy Geographic Routing Algorithms

Guoliang Xing, *Student Member, IEEE*, Chenyang Lu, *Member, IEEE*,
Robert Pless, *Member, IEEE*, and Qingfeng Huang, *Member, IEEE*

Abstract—Greedy geographic routing is an attractive localized routing scheme for wireless sensor networks due to its efficiency and scalability. However, greedy geographic routing may fail due to routing voids on random network topologies. We study greedy geographic routing in an important class of wireless sensor networks (e.g., surveillance or object tracking systems) that provide sensing coverage over a geographic area. Our analysis and simulation results demonstrate that an existing geographic routing algorithm, greedy forwarding (GF), can successfully find short routing paths based on local states in sensing-covered networks. In particular, we derive theoretical upper bounds on the network dilation of sensing-covered networks under GF. We also propose a new greedy geographic routing algorithm called Bounded Voronoi Greedy Forwarding (BVGF) that achieves path dilation lower than 4.62 in sensing-covered networks as long as the communication range is at least twice the sensing range. Furthermore, we extend GF and BVGF to achieve provable performance bounds in terms of total number of transmissions and reliability in lossy networks.

Index Terms—Sensor networks, coverage, geographic routing, greedy routing, wireless communication.

1 INTRODUCTION

WIRELESS sensor networks represent a new type of ad hoc networks that integrate sensing, processing, and wireless communication in a distributed system. While sensor networks have many similarities with traditional ad hoc networks, such as those comprised of laptops, they also face new requirements introduced by their distributed sensing applications. In particular, many critical applications (e.g., distributed detection [32], distributed tracking and classification [20]) of sensor networks introduce the fundamental requirement of *sensing coverage* that does not exist in traditional ad hoc networks. In a sensing-covered network, every point in a geographic area of interest must be within the sensing range of at least one sensor.

The problem of providing sensing coverage has received significant attention. Several algorithms [7], [5], [24], [39] were proposed to achieve sensing coverage when a sensor network is deployed. Other projects [31], [33], [37], [38] developed online energy conservation protocols that dynamically maintain sensing coverage using only a subset of nodes. Complimentary to existing research on coverage provisioning and geographic routing on random network topologies, we study the impact of sensing coverage on the performance of *greedy geographic routing* in wireless sensor networks.

Geographic routing is a suitable routing scheme in sensor networks. Unlike IP networks, communication in

sensor networks is often addressed by physical locations. For example, instead of querying a sensor with a particular ID, a user often queries a geographic region. The identities of sensors that happen to be located in that region are not important. Any node in that region that receives the query may participate in data aggregation and reports the result back to the user. This location-centric communication paradigm allows geographic routing to be performed without incurring the overhead of location directory services [21]. Furthermore, geographic routing makes efficient routing decisions based on local states (e.g., locations of one-hop neighbors). This localized nature enables it to scale well in large distributed microsensing applications.

As the simplest form of geographic routing, greedy forwarding (GF) is particularly attractive in sensor networks. In this paper, GF refers to a simple routing scheme in which a node always forwards a packet to the neighbor that has the shortest distance¹ to the destination. Due to the low overhead, GF can be easily implemented on resource constrained sensor network platforms. However, earlier research has shown that GF often fails due to routing voids on random network topologies. In this paper, we present new geometric analysis and simulation results that demonstrate, GF is a viable and effective routing scheme in sensing-covered networks deployed in convex regions. Specifically, the key results in this paper include the following.

1. We establish a constant upper bound on the network dilation of sensing-covered networks based on Delaunay Triangulations in Section 4.
2. We then derive a new upper bound on network dilation for sensing-covered networks under GF in

1. Different definitions of distance (e.g., Euclidean distance or projected distance on the straight line toward the destination) may be adopted by different algorithms.

• G. Xing, C. Lu, and R. Pless are with the Department of Computer Science and Engineering, Washington University in St. Louis, One Brookings Drive, St. Louis, MO 63130. E-mail: {xing, lu, pless}@cse.wustl.edu.
• Q. Huang is with Palo Alto Research Center (PARC) Inc., 3333 Coyote Hill Road, Palo Alto, CA 94304. E-mail: qhuang@parc.com.

Manuscript received 16 Feb. 2005; revised 23 Apr. 2005; accepted 9 June 2005; published online 24 Feb. 2006.

Recommended for acceptance by I. Stojmenovic, S. Olariu, and D. Simplot-Ryl.

For information on obtaining reprints of this article, please send e-mail to: tpd@computer.org, and reference IEEECS Log Number TPDI-0145-0205.

Section 5. This bound monotonically decreases as the network's range ratio (the communication range divided by the sensing range) increases.

3. We also propose a new greedy geographic routing algorithm called Bounded Voronoi Greedy Forwarding (BVGF) that achieves a lower bound on network dilation than GF (see Section 6).
4. We extend GF and BVGF to handle unreliable communication links which are common in real wireless sensor networks. These variants of GF and BVGF have analytical bounds in terms of total number of transmissions and path reliability in lossy networks (see Section 7).
5. Finally, our theoretical results are validated through simulations based on both a deterministic radio model and a realistic model of Mica2 motes (see Section 8).

2 RELATED WORK

Routing in ad hoc wireless (sensor) networks has been studied extensively in the past decade. The most relevant works include various geographic routing algorithms [23], [29], [4], [16], [30].

As the simplest form of geographic routing, greedy forwarding (GF) makes routing decisions only based on the locations of a node's one-hop neighbors, thereby avoiding the overhead of maintaining global topology information. GF always chooses a next hop that minimizes a certain routing metric. Several routing metrics have been proposed for GF, which include the Euclidean distance to the destination [12], the projected distance to the destination (on the straight line joining the current node and the destination) [30], and the direction to the destination (measured by the angle between the straight line joining the current node and the destination and the straight line joining a neighbor and the destination) [17]. However, GF may fail if a node encounters local minima, when it cannot find a "better" neighbor than itself. Previous studies found that such local minima are prevalent in ad hoc networks. Several schemes have been proposed to recover from the local minima. GFG [4], GPSR [16], and GOAFR+ [18] route a packet around the faces of a planar subgraph extracted from the original network, while limited flooding is used in [29] to circumvent local minima. To guarantee delivery, many existing geographic routing algorithms (e.g., GFG [4], GPSR [16], GOAFR+ [18], and the routing schemes proposed in [29]) switch between the GF mode and recovery mode depending on the network topology. Unfortunately, the recovery mode inevitably introduces additional overhead and complexity to geographic routing algorithms.

The stretch factors of specific geometric topologies have been studied for wireless networks. The recovery algorithm in GPSR [16] routes packets around the faces of one of two planar subgraphs, namely, *Relative Neighborhood Graph* (RNG) and *Gabriel Graph* (GG), to escape from routing voids. However GG and RNG are not good spanners of the original graph [11], i.e., two nodes that are a few hops away in the original network might be very far apart in GG and RNG. The *Delaunay Triangulation* (DT) has been shown to be a good spanner with a constant stretch factor [9], [15], [6]. The probabilistic bound on the Euclidean length of DT paths constructed with respect to a Poisson point process is analyzed in [2]. However, the DT of a random network

topology may contain arbitrarily long edges which exceed limited wireless transmission range. To enable the local routing algorithms to leverage on the good spanning property of DT, two distributed algorithms for constructing local approximations of the DT are proposed in [13], [22]. Interestingly, these local approximations to DT are also good spanners with the same constant stretch factor as DT. However, finding the routing paths with bounded length in DT requires global topology information [9]. The Parallel Voronoi Routing (PVR) [3] algorithm deals with this problem by exploring the parallel routes which may have bounded lengths. Unlike the existing works that assume arbitrary node distribution, our work focuses on the greedy geographic routing on *sensing-covered* topologies.

3 PRELIMINARIES

3.1 Assumptions

We assume all sensor nodes are located in a two-dimensional space. Every node has the same sensing range R_s . For a node located at point p , we use circle $C(p, R_s)$ that is centered at point p and has a radius R_s to represent the *sensing circle* of the node. A node can *cover* any point inside its sensing circle. We assume that a node does not cover the points *on* its sensing circle. While this assumption has little impact on the performance of a sensor network in practice, it simplifies our theoretical analysis. We assume the deployment region of a sensor network is convex. A network is *sensing-covered* if any point in the deployment region of the network is covered by at least one node.

We assume a deterministic communication model in our first set of analysis. In this model, any two nodes u and v can directly communicate with each other if and only if $|uv| \leq R_c$, where $|uv|$ is the Euclidean distance between u and v , and R_c is the communication range of the network. Under this model, a network can be represented by a *unit disk graph* $G(V, E)$, where V represents the set of nodes in the network and an edge $(u, v) \in E$ if and only if $|uv| \leq R_c$. In Section 7, we extend the algorithms and analysis based on the deterministic model to a probabilistic communication model that captures the characteristics of unreliable sensor networks.

3.2 Double Range Property

The ratio between the communication range, R_c , and the sensing range, R_s , has a significant impact on the achievable routing quality of a sensing-covered network. In this paper, we call R_c/R_s the *range ratio*. Intuitively, as the range ratio increases, a sensing-covered network becomes denser, resulting in better routing quality.

In practice, both communication and sensing ranges are highly dependent on the system platform, the application, and the environment. The communication range of a wireless network interface depends on the property of radio (e.g., transmission power, baseband/wide-band, and antenna) and the environment (e.g., indoor or outdoor) [40]. The outdoor radio ranges of several wireless (sensor) network interfaces are listed in Table 1.²

The sensing range of a sensor network depends on the sensor modality, sensor design, and the requirements of

2. The empirical study [40] shows that the effective radio range of the Mica1 mote varies with the environment and usually is shorter than the specification.

TABLE 1

The Radio Ranges of Wireless Network Platforms [8], [27], [28]

Platforms	Mica1 mote	Mica2 mote	Sensoria SGate	802.11b (SonicWall)
R_c (ft)	100	1000	1640	1200 ~ 2320

specific sensing applications. The sensing range has a significant impact on the performance of a sensing application and is usually determined empirically to satisfy the Signal-to-Noise Ratio (SNR) required by the application. For example, the empirical results in [10] showed that the performance of target classification degrades quickly with the distance between a sensor and a target. In their real-world experiments on sGate [27], a sensor platform from Sensoria Corp., different types of military vehicles drove through the sensor deployment region and the types of the vehicles were identified based on the acoustic measurements. The experimental results showed that the probability of correct vehicle classification decreases quickly with the sensor-target distance and drops below 50 percent when the sensor-target distance exceeds 100m. Hence, the effective sensing range is much shorter than 100m. The experiments for a similar application [14] showed that the sensing range of seismic sensors is about 50m.

Clearly, the range ratio varies across a wide range due to the heterogeneity of sensor networks. As a starting point for the analysis, in this paper, we focus on those networks with the *double range property*, i.e., $R_c/R_s \geq 2$. This assumption is motivated by the geometric analysis in [33], which showed that a sensing-covered network is always connected if it has the double range property. Since network connectivity is necessary for any routing algorithm to find a routing path, it is reasonable to assume the double-range property as a starting point.

Empirical experiences have shown that the double range property is applicable to a number of representative sensing applications. For example, the aforementioned sGate-based network used for target classification [10] has a sensing range $R_s < 100m$, and communication range $R_c = 1,640ft$ (547m) (as shown in Table 1), which corresponds to a range ratio $R_c/R_s > 5.47$. The double range property will also hold if the seismic sensors used in [14] are combined with a wireless network interface that has a communication range $R_c \geq 100m$.

All results and analyses in the rest of this paper assume that a sensor network is deployed in a convex region and has the double property unless otherwise stated.

3.3 Metrics

The performance of a routing algorithm can be characterized by the *network length* (i.e., hop count) and *Euclidean length* (i.e., the sum of the Euclidean distance of each hop) of the routing paths it finds. Note the path with the shortest network length may be different from the path with the shortest Euclidean length. In this paper, we focus more on the network length. Network length has a significant impact on the delay and the throughput of multihop ad hoc networks. A routing algorithm that can find the paths with short Euclidean length may potentially reduce the network

energy consumption by controlling the transmission power of the wireless nodes [25], [34].

The performance of a routing algorithm is inherently affected by the path quality of the underlying networks. *Stretch factor* [11] is an important metric for comparing the path quality between two graphs. Let $\tau_G(u, v)$ and $d_G(u, v)$ represent the shortest network and Euclidean length between nodes u and v in graph $G(V, E)$, respectively. A subgraph $H(V, E')$, where $E' \subseteq E$, is a *network t -spanner* of graph $G(V, E)$ if $\forall u, v \in V, \tau_H(u, v) \leq t \cdot \tau_G(u, v)$. Similarly, $H(V, E')$ is an *Euclidean t -spanner* of graph $G(V, E)$ if $\forall u, v \in V, d_H(u, v) \leq t \cdot d_G(u, v)$, where t is called the *network (Euclidean) stretch factor* of the spanner $H(V, E')$.

In this paper, we use *dilation* to represent the stretch factor of the wireless network $G(V, E)$ relative to an *ideal* wireless network in which there exists a path with network length $\lceil \frac{|uv|}{R_c} \rceil$ and a path with Euclidean length $|uv|$ for any two nodes u and v . We define the following two dilations:

Definition 1. The *network dilation* of the network $G(V, E)$ is defined by:

$$D_n = \max_{u, v \in V} \frac{\tau_G(u, v)}{\lceil \frac{|uv|}{R_c} \rceil}.$$

Definition 2. The *Euclidean dilation* of the network $G(V, E)$ is defined by:

$$D_e = \max_{u, v \in V} \frac{d_G(u, v)}{|uv|}.$$

We note that Euclidean dilation has been widely used in graph theory to characterize the quality of a graph [11]. Clearly, the dilation of a wireless network is an upper bound of the stretch factor relative to *any* possible wireless network composed of the same set of nodes. *Asymptotic network dilation* (denoted by \bar{D}_n) is the value that the network dilation converges to when the network length approaches infinity. Asymptotic network dilation is useful in characterizing the path quality of a large-scale wireless network. We say $D_n(R)$ is the *network dilation of the wireless network $G(V, E)$ under routing algorithm R* (or *network dilation of R* for abbreviation) if $\tau_G(u, v)$ in Definition 1 represents the network length of the routing path between nodes u and v chosen by R . The network dilation of a routing algorithm characterizes the performance of the algorithm relative to the *ideal* case in which the path between any two nodes u and v has $\lceil \frac{|uv|}{R_c} \rceil$ hops. The Euclidean dilation of R is defined similarly.

4 DILATION ANALYSIS BASED ON DT

In this section, we study the dilation property of sensing-covered networks based on Delaunay Triangulations (DT). We first show that the DT of a sensing-covered network is a subgraph of the network when the double-range property holds. We then quantify the Euclidean and network dilations of sensing-covered networks.

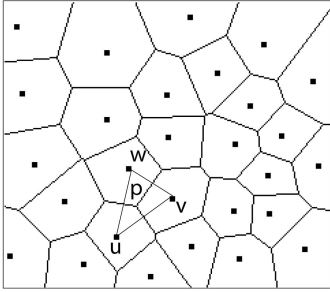


Fig. 1. The Voronoi diagram of a sensing-covered network.

4.1 Voronoi Diagram and Delaunay Triangulation

For a set of n nodes V in 2D space, the Voronoi diagram of V is the partition of the plane into n Voronoi regions, one for each node in V . The Voronoi region of node i ($i \in V$) is denoted by $Vor(i)$. Fig. 1 shows a Voronoi diagram of a set of nodes. A point in the plane lies in $Vor(i)$ if and only if i is the closest node to the point. The boundary between two contiguous Voronoi regions is called a Voronoi edge. A Voronoi edge is on the perpendicular bisector of the segment connecting two adjacent nodes. A Voronoi vertex is the intersection of Voronoi edges. As shown in Fig. 1, point p is a Voronoi vertex of three contiguous Voronoi regions: $Vor(u)$, $Vor(v)$, and $Vor(w)$. We assume that all nodes are in *general positions*, that is, no three nodes lie on the same straight line and no four nodes lie on the same circle.

In the dual graph of a Voronoi diagram, Delaunay Triangulation (denoted by $DT(V)$), there is an edge between nodes u and v in $DT(V)$ if and only if the Voronoi regions of nodes u and v share a boundary. $DT(V)$ consists of *Delaunay triangles*. $DT(V)$ is planar, i.e., no two edges cross. It has been shown in [9] that the Delaunay Triangulation is a good Euclidean spanner of the complete Euclidean graph. The upper bound of the Euclidean stretch factor is $\frac{1+\sqrt{5}}{2}\pi$ [9]. A tighter bound on the stretch factor, $\frac{4\sqrt{3}}{9}\pi \approx 2.42$, is proved in [15].

4.2 Dilation Property

In this section, we investigate the Euclidean and network dilations of sensing-covered networks. We first study the properties of Voronoi diagrams and DT of sensing-covered networks. These results lead to bounded dilations of such networks.

In a sensing-covered network deployed in a convex region A , the Voronoi region of a node located at the vicinity of A 's boundary may exceed the boundary of A or even be unbounded. In the rest of this paper, we only consider the partial Voronoi diagram that is bounded by the deployment region A and the corresponding dual graph. As illustrated in Fig. 1, the Voronoi region of any node in this partial Voronoi diagram is contained in the region A . Consequently, the dual graph of this partial Voronoi diagram is a partial DT that does not contain the edges between any two nodes whose Voronoi regions (of the original Voronoi diagram) join outside A .

In a sensing-covered convex region, any point is covered by the node closest to it. This simple observation leads to the following lemma:

Lemma 1 (Coverage Lemma). *A convex region A is covered by a set of nodes V if and only if each node can cover its Voronoi region (including the boundary).*

Proof. The nodes partition the convex region A into a number of Voronoi regions in the Voronoi diagram. Clearly, if each Voronoi region (including the boundary) is covered by the node within it, region A is sensing-covered. On the other hand, if region A is covered, any point in region A must be covered by the *closest* node(s) to it. In the Voronoi diagram, all the points in a Voronoi region share the same closest node. Thus, every node can cover all the points in its Voronoi region. Any point on the boundary of two Voronoi regions $Vor(i)$ and $Vor(j)$ has the same distance from i and j and is covered by both of them. \square

According to Lemma 1, every Voronoi region $Vor(u)$ in a sensing-covered network is contained in the sensing circle of u . This property results in the following lemma:

Lemma 2. *In a sensing-covered network $G(V, E)$ deployed in a convex region A , the Delaunay Triangulation of the nodes is a subgraph of the network, i.e., $DT(V) \subseteq G(V, E)$. Furthermore, any DT edge is shorter than $2R_s$.*

Proof. It is clear that the two graphs $DT(V)$ and $G(V, E)$ share the same set of vertices. We now show that any DT edge between u and v is also an edge in $G(V, E)$. As illustrated in Fig. 1, the Voronoi vertex p is the intersection of three contiguous Voronoi regions, $Vor(u)$, $Vor(v)$, and $Vor(w)$. From Lemma 1, p is covered by u , v , and w . Hence, $|pu|$, $|pv|$, and $|pw|$ are all less than R_s . Thus, according to the triangle inequality, $|uw| \leq |up| + |pv| < 2R_s$. From the double range property, we have $|uw| < R_c$. Therefore, uw is an edge of $G(V, E)$. \square

Since the unit disk graph of a sensing-covered network contains the DT of the nodes, the dilation property of a sensing-covered network is at least as good as DT.

Theorem 1. *A sensing-covered network $G(V, E)$ has a Euclidean dilation $\frac{4\sqrt{3}}{9}\pi$, i.e., $\forall u, v \in V, d_G(u, v) \leq \frac{4\sqrt{3}}{9}\pi|uw|$.*

Proof. As proved in [15], the upper bound on the stretch factor of DT is $\frac{4\sqrt{3}}{9}\pi$. From Lemma 2, $DT(V) \subseteq G(V, E)$, thus $\forall u, v \in V, d_G(u, v) \leq d_{DT}(u, v) \leq \frac{4\sqrt{3}}{9}\pi|uw|$. \square

In addition to the competitive Euclidean dilation shown by Theorem 1, we next show that a sensing-covered network also has a good network dilation.

Theorem 2. *In a sensing-covered network $G(V, E)$, the network length of the shortest path between node u and v satisfies:*

$$\tau_G(u, v) \leq \left\lfloor \frac{8\pi\sqrt{3}}{9} \cdot \frac{|uw|}{R_c} \right\rfloor + 1.$$

Proof. Clearly, the theorem holds if u and v are adjacent in $G(V, E)$. Now, we consider the case where the network length between u and v is at least 2. Let Π represent the path in $G(V, E)$ that has the shortest Euclidean length between nodes u and v . Let N be the network length of Π . Consider three consecutive nodes s_i , s_{i+1} , and s_{i+2} on Π , as shown in Fig. 2. Clearly, there is no edge between s_i and s_{i+2} in $G(V, E)$ because, otherwise, choosing s_{i+2} as the next hop of s_i results in a path with shorter Euclidean

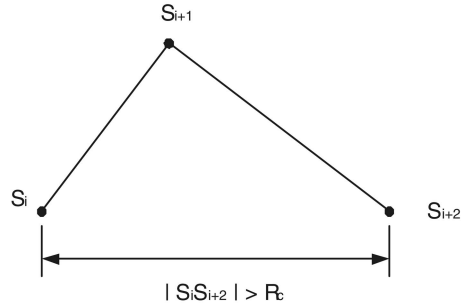


Fig. 2. Three consecutive nodes on a path.

length than Π , which contradicts the assumption that Π is the path with the shortest Euclidean length between u and v . Hence, $|s_i s_{i+2}| > R_c$. From the triangle inequality, $|s_i s_{i+1}| + |s_{i+1} s_{i+2}| \geq |s_i s_{i+2}| > R_c$. Summing this inequality over consecutive hops on the path, we have:

$$R_c \left\lfloor \frac{N}{2} \right\rfloor < d_G(u, v). \quad (1)$$

From Theorem 1, we have

$$d_G(u, v) \leq \frac{4\sqrt{3}\pi R_c}{9} \frac{|uv|}{R_c}. \quad (2)$$

From (1) and (2), the shortest network length satisfies:

$$\tau_G(u, v) \leq N \leq \left\lceil \frac{8\pi\sqrt{3}}{9} \cdot \frac{|uv|}{R_c} \right\rceil + 1. \quad \square$$

The asymptotic bound on the network dilation of sensing-covered networks can be obtained by ignoring the rounding and constant term 1 in $\tau_G(u, v)$ defined in Theorem 2.

Corollary 1. *The asymptotic network dilation of sensing-covered networks is $\frac{8\sqrt{3}\pi}{9}$.*

Theorem 1 and Corollary 1 show that the sensing-covered networks have good Euclidean and network dilation properties.

We note that the analysis in this section only considers the DT subgraph of the network and ignores any communication edge that is not a DT edge. When R_c/R_s is large, a DT edge in a sensing-covered network can be significantly shorter than R_c , and the dilation-bounds-based DT can be very conservative. In the following sections, we will show that significantly tighter dilation bounds are achieved by greedy routing algorithms such as GF when R_c/R_s becomes higher.

5 GREEDY FORWARDING

In this section, we prove that GF always succeeds in sensing-covered networks when the double-range property is satisfied and, hence, the delivery of a packet is guaranteed without complex recovery modes. We further derive the upper bound on the network dilation of sensing-covered networks under GF. As discussed in Section 2, several different routing metrics can be used in GF. In this section, we focus on the Euclidean distance and the projected distance metrics.

Theorem 3. *In a sensing-covered network, GF can always find a routing path between any two nodes. Furthermore, in each step*

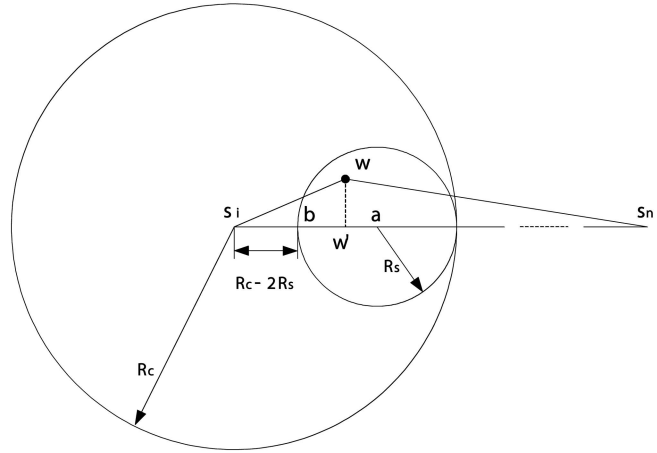


Fig. 3. GF always finds a next-hop node.

(other than the last step arriving at the destination), a node can always find a next-hop node that is more than $R_c - 2R_s$ closer (in terms of both Euclidean and projected distance) to the destination than itself.

Proof. Let s_n be the destination and s_i be either the source or an intermediate node on the GF routing path, as shown in Fig. 3. If $|s_i s_n| \leq R_c$, s_n is reached in one hop. If $|s_i s_n| > R_c$, we find point a on $\overline{s_i s_n}$ such that $|s_i a| = R_c - R_s$. Since $R_c \geq 2R_s$, point a must be outside of the sensing circle of s_i . Since a is covered, there must be at least one node, say w , inside the circle $C(a, R_s)$.

We now prove that the progress toward s_n (in terms of both Euclidean and projected distance) is more than $R_c - 2R_s$ by choosing w as the next hop of s_i . Let point b be the intersection between $\overline{s_i s_n}$ and $C(a, R_s)$ that is closest to s_i . Since circle $C(a, R_s)$ is internally tangent with the communication circle of node s_i , $|s_i b| = R_c - 2R_s$. Clearly, the maximal distance between s_n and any point on or inside $C(a, R_s)$ is $|s_n b|$. Suppose w' is the projection of node w on line segment $\overline{s_i s_n}$. We have: $|s_n s_i| - |s_n w'| \geq |s_n s_i| - |s_n w| > |s_i b| = R_c - 2R_s \geq 0$.

From above relation, we can see that both the projected distance and the Euclidean distance in one hop (other than the last hop arriving at the destination) of a GF routing path is more than $R_c - 2R_s$. Thus, GF can always find a routing path between any two nodes. \square

Theorem 3 establishes that the progress toward the destination in each step of a GF routing path is lower-bounded by $R_c - 2R_s$. As a result, the following theorem shows that the network length of a GF path is upper-bounded. The proof is presented in [36] and not included here due to space limitation.

Theorem 4. *In a sensing-covered network, GF can always find a routing path between source u and destination v no longer than $\left\lceil \frac{|uv|}{R_c - 2R_s} \right\rceil + 1$ hops.*

From Theorem 4 and Definition 1, the network dilation of a network $G(V, E)$ under GF satisfies:

$$D_n(GF) \leq \max_{u, v \in V} \left(\frac{\left\lceil \frac{|uv|}{R_c - 2R_s} \right\rceil + 1}{\left\lceil \frac{|uv|}{R_c} \right\rceil} \right). \quad (3)$$

The *asymptotic* network dilation bound of sensing-covered networks under GF can be computed by ignoring the rounding and the constant term 1 in (3).

Corollary 2. *The asymptotic network dilation of sensing-covered networks under GF satisfies*

$$\tilde{D}_n(GF) \leq \frac{R_c}{R_c - 2R_s}. \quad (4)$$

From (4), the dilation upper bound monotonically decreases when R_c/R_s increases. It becomes lower than 2 when $R_c/R_s > 4$ and approaches 1 when R_c/R_s becomes very large. This result confirms our intuition that a sensing-covered network approaches an ideal network in terms of network length when the communication range is significantly longer than the sensing range.

However, the GF dilation bound in (4) increases quickly to infinity when R_c/R_s approaches 2. In the proof of Theorem 3, when R_c approaches $2R_s$, a forwarding node s_i may be infinitely close to the intersection point between $C(a, R_s)$ and $\overline{s_i s_n}$. Consequently, s_i may choose a neighbor inside $C(a, R_s)$ that makes an infinitely small progress toward the destination and, hence, results in a long routing path. Similar to the proof of Theorem 5.1 in [13], it can be shown that the network length of a GF routing path between source u and destination v is bounded by $O((\frac{|uv|}{R_c})^2)$. From Definition 1, we can see that this result cannot lead to a constant upper bound on the network dilation for a given range ratio. Whether GF has a tighter analytical network dilation bound when R_c/R_s is close to two is an open research question left for future work.

6 BOUNDED VORONOI GREEDY FORWARDING (BVGF)

We note that, although GF has a satisfactory network dilation bound when $R_c/R_s \gg 2$, the bound becomes very large when R_c/R_s is close to two. In contrast, the analysis based on the Voronoi diagram in Section 4 leads to a satisfactory bound when R_c/R_s is close to two, but this bound becomes conservative when $R_c/R_s \gg 2$. These results motivate us to develop a new routing algorithm, Bounded Voronoi Greedy Forwarding (BVGF), that has a satisfactory analytical dilation bound for any $R_c/R_s > 2$ by combining GF and the Voronoi diagram.

6.1 The BVGF Algorithm

Similar to GF, BVGF is a localized algorithm that makes greedy routing decisions based on one-hop neighbor locations. When node i needs to forward a packet, a neighbor j is eligible as the next hop only if the line segment joining the source and the destination intersects $Vor(j)$ or coincides with one of the boundaries of $Vor(j)$. BVGF chooses as the next hop the neighbor that has the shortest Euclidean distance to the destination among all eligible neighbors. When there are multiple eligible neighbors that are equally closest to the destination, the routing node randomly chooses one as the next hop. Fig. 4 illustrates four consecutive nodes ($s_i s_{i+3}$) on the BVGF routing path from

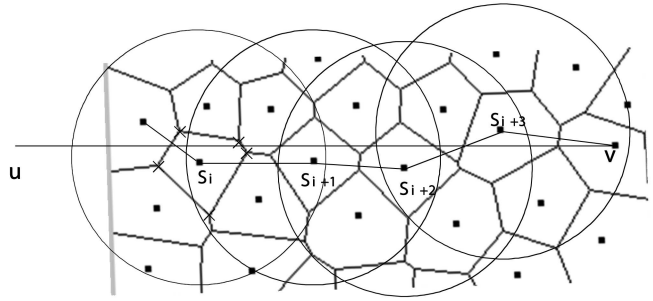


Fig. 4. A routing path of BVGF.

source u to destination v . The communication circle of each node is also shown in the figure. We can see that a node's next hop on a routing path might not be adjacent with it in the Voronoi diagram (e.g., node s_i does not share a Voronoi edge with node s_{i+1}). When $R_c \gg R_s$, this greedy forwarding scheme allows BVGF to achieve a tighter dilation bound than the DT bound that only considers DT edges and does not vary with the range ratio.

The key difference between GF and BVGF is that BVGF only considers the neighbors whose Voronoi regions are intersected by the line joining source and destination. As we will show later in this section, this feature allows BVGF to achieve a tighter upper-bound on the network dilation.

In BVGF, each node maintains a neighborhood table. For each one-hop neighbor j , the table includes j 's location and the locations of the vertices of $Vor(j)$. For example, as shown in Fig. 4, for one-hop neighbor s_i , node s_{i+1} includes in its neighborhood table the locations of s_i and the vertices of $Vor(s_i)$ (denoted by crosses). To maintain the neighborhood table, each node periodically broadcasts a beacon message that includes its location and the locations of the vertices of its Voronoi region. Note that each node can compute its own Voronoi vertices based on its neighbor locations since all Voronoi neighbors are within its communication range (as proved in Lemma 2).

Suppose the number of nodes within a node's communication range is bounded by $O(n)$. The number of Voronoi vertices within a node's neighborhood is bounded by $O(n)$ [1]. Hence, both the size of a beacon message and a node's neighborhood table are bounded by $O(nL)$, where L is the number of bits used to represent a location. The time complexity incurred by a node to compute the Voronoi diagram of all its neighbors is $O(n \log n)$ [1].

6.2 Network Dilation of BVGF

In this section, we analyze the network dilation of BVGF. To simplify our discussion on the routing path from source u to destination v , we assume node u is the origin and the straight line joining u and v is the x -axis. The *Voronoi forwarding rectangle* of nodes u and v refers to the rectangle defined by the points $(0, R_s)$, $(0, -R_s)$, $(|uv|, -R_s)$, and $(|uv|, R_s)$. Let $x(a)$ and $y(a)$ denote the x -coordinate and y -coordinate of a point a , respectively. The projected progress between two nodes is defined as the difference between their x -coordinates.

We first prove that BVGF can find a routing path between any two nodes in a sensing-covered network (Theorem 5). We next show that a BVGF routing path

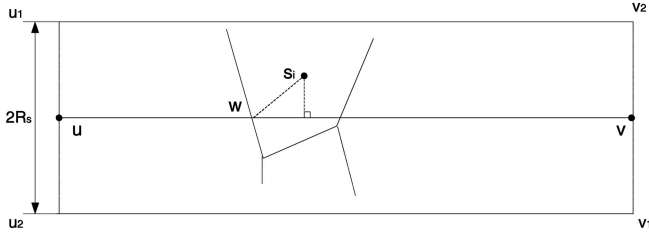


Fig. 5. Voronoi forwarding rectangle.

always lies in the Voronoi forwarding rectangle. We then derive lower bounds on the projected progress in every step of a BVGF path (Lemma 4). Since this lower bound is not tight when R_c/R_s is close to two, we derive tighter lower bounds on the projected progress in two and four consecutive steps on a BVGF path (Lemmas 6 and 7). Finally, we establish the asymptotic bounds of the network dilation of BVGF in Theorem 7.

At each step, BVGF chooses the next-hop node whose Voronoi region is intersected by the x -axis, which can lead to a routing path to the destination composed of nodes close to the x -axis. We have the following theorem. The proof is presented in [36] and not included here due to space limitation.

Theorem 5. *In a sensing-covered network, BVGF can always find a routing path between any two nodes. Furthermore, the projected progress at each step of BVGF is positive.*

BVGF always forwards a packet to a node whose Voronoi region is intersected by the x -axis. Using this property, combined with the fact that every Voronoi region is bounded by a sensing circle (Lemma 1), we can prove that any node on a BVGF routing path lies in the Voronoi rectangle. As shown in Fig. 5, s_i is an intermediate node on the BVGF routing path between u and v . Let point w be one of the intersections between the x -axis and $Vor(s_i)$ (if x -axis coincides with one of the boundaries of $Vor(s_i)$, choose a vertex on the boundary as point w). From Lemma 1, every Voronoi region is within a sensing circle. That is, node s_i covers point w . Hence, $|y(s_i)| \leq |s_i w| < R_s$. Furthermore, from Theorem 5, $0 < |x(s_i)| < |uw|$. The above discussion proves the following lemma:

Lemma 3. *The BVGF routing path from node u to node v lies in the Voronoi forwarding rectangle of nodes u and v .*

In a sensing-covered network, the greedy nature of BVGF ensures that a node chooses a next hop that has the shortest distance to the destination among all eligible neighbors. On the other hand, according to Lemma 3, the next-hop node must fall in the Voronoi forwarding rectangle. These results allow us to derive a lower bound on the progress of every step of BVGF.

Lemma 4 (One-step Advance Lemma). *In a sensing-covered network, the projected progress in each step of a BVGF routing path is more than Δ_1 , where $\Delta_1 = \max(0, \sqrt{R_c^2 - 2R_c R_s} - R_s)$.*

Proof. As illustrated in Fig. 6, s_i is an intermediate node on the BVGF routing path between source u and

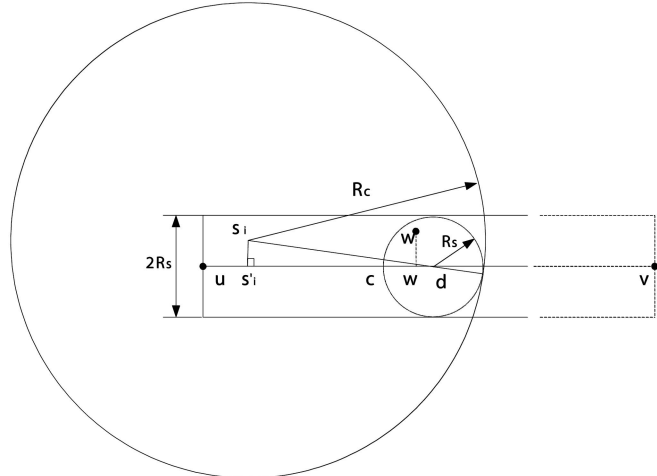


Fig. 6. One-step projected progress.

destination v . Let point s'_i be the projection of s_i on the x -axis. From Lemma 3, $s_i s'_i < R_s$. Let point d be the point on the x -axis such that $|s_i d| = R_c - R_s$. According to Lemma 1, there must exist a node, w , which covers point d and $d \in Vor(w)$. Clearly, w lies in circle $C(d, R_s)$. Since d is on the x -axis and $d \in Vor(w)$, the x -axis intersects $Vor(w)$. Furthermore, since circle $C(d, R_s)$ is internally tangent with the communication circle of node s_i , node w is within the communication range of node s_i . Therefore, node s_i can at least choose node w as the next hop. Let c be the intersection between $C(d, R_s)$ and the x -axis that is closest to u . Let w' be the projection of w on the x -axis. The projected progress between s_i and w is:

$$\begin{aligned} |s'_i w'| &> |s'_i c| = |s'_i d| - R_s = \sqrt{|s_i d|^2 - |s_i s'_i|^2} - R_s \\ &> \sqrt{(R_c - R_s)^2 - R_s^2} - R_s = \sqrt{R_c^2 - 2R_c R_s} - R_s. \end{aligned}$$

$\sqrt{R_c^2 - 2R_c R_s} - R_s \leq 0$ when $R_c/R_s \leq 1 + \sqrt{2}$. From Theorem 5, projected progress made by BVGF in each step is positive. Therefore, the projected progress in each step is lower-bounded by $\max(0, \sqrt{R_c^2 - 2R_c R_s} - R_s)$. \square

Lemma 4 shows that the projected progress between any two nodes on a BVGF routing path may approach zero when $R_c/R_s \leq 1 + \sqrt{2}$. We ask the question whether there is a tighter lower bound in such a case. Consider two nonadjacent nodes i and j on a BVGF routing path. The Euclidean distance between them must be longer than R_c because, otherwise, BVGF would have chosen j as the next hop of i , which contradicts the assumption that i and j are nonadjacent on the routing path. We refer to this property of BVGF as the *nonadjacent advancing property*.³ We have the following lemma:

Lemma 5 (Nonadjacent Advancing Property). *In a sensing-covered network, the Euclidean distance between any two nonadjacent nodes on a BVGF routing path is longer than R_c .*

Lemma 5, combined with the fact that a BVGF path lies in the Voronoi forwarding rectangle, leads to the intuition

3. Similarly, GF also can be shown to have this property.

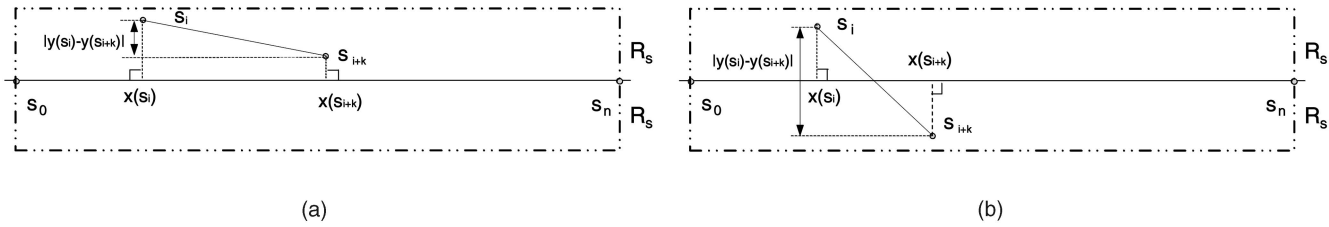


Fig. 7. Projected progress of two nonadjacent nodes.

that the projected progress toward the destination made by BVGF in two consecutive steps is lower-bounded. We have the following lemma that establishes a tighter bound on the projected progress of BVGF than Lemma 4 when R_c/R_s is small:

Lemma 6 (Two-Step Advance Lemma). *In a sensing-covered network, the projected progress between any two nonadjacent nodes i and j on a BVGF routing path is more than $\Delta_2 = \sqrt{R_c^2 - 4R_s^2}$.*

Proof. Let $s_0(u), s_1 \dots s_{n-1}, s_n(v)$ be the consecutive nodes on the BVGF routing path between u and v . From Lemma 5, $|s_i s_{i+k}| > R_c$ ($k > 1$). Fig. 7a and Fig. 7b illustrate the two cases where s_i and s_{i+k} are on the same or different sides of the x -axis, respectively. Both s_i and s_{i+k} lie in the Voronoi forwarding rectangle of nodes u and v (dotted box in the figure). When s_i and s_{i+k} are on the same side of the x -axis, then $|y(s_{i+k}) - y(s_i)| < R_s$. The projected progress between them satisfies:

$$x(s_{i+k}) - x(s_i) = \sqrt{|s_i s_{i+k}|^2 - (y(s_{i+k}) - y(s_i))^2} > \sqrt{R_c^2 - R_s^2}.$$

Similarly, when s_i and s_{i+k} are on different sides of the x -axis as shown in Fig. 7b, we can prove that $x(s_{i+k}) - x(s_i) \geq \sqrt{R_c^2 - 4R_s^2}$. Summarizing the results of the above two cases, the minimum projected progress between any two nonadjacent nodes is $\sqrt{R_c^2 - 4R_s^2}$. \square

Considering the different cases of nonadjacent node locations, we can further derive the lower bound on the projected progress made by BVGF in four consecutive steps. We have the following theorem (the proof is presented in [36] and not included here due to space limitation):

Lemma 7 (Four-Step Advance Lemma). *In a sensing-covered network, the projected progress in four consecutive steps of a BVGF routing path is more than Δ_4 , where*

$$\Delta_4 = \begin{cases} \sqrt{R_c^2 - R_s^2} & (2 \leq R_c/R_s \leq \sqrt{5}) \\ \sqrt{4R_c^2 - 16R_s^2} & (R_c/R_s > \sqrt{5}). \end{cases}$$

When R_c/R_s is small, the network is relatively sparse. Although the one-step projected progress approaches zero as shown in Lemma 4, in such a case, interestingly, Lemmas 6 and 7 show that the projected progress toward the destination made by BVGF in two or four consecutive steps is lower-bounded. On the other hand, when $R_c \gg R_s$, the sensing coverage of the network can result in a high density of nodes in the communication range of a routing node and, hence, the projected progress of BVGF in each step approaches R_c . In such a case, the lower bound

established in Lemma 4 is tighter than the lower bounds established in Lemmas 6 and 7.

Based on the one-hop, two-hop, and four-hop minimum projected progress derived in Lemmas 4, 6, and 7, respectively, we can derive the upper bounds on the network length of a BVGF routing path. Summarizing these upper bounds, we have the following theorem:

Theorem 6. *In a sensing-covered network, the BVGF routing path between any two nodes u and v is no longer than Δ hops, where*

$$\Delta = \min \left\{ \left\lceil \frac{|uv|}{\Delta_1} \right\rceil, 2 \left\lceil \frac{|uv|}{\Delta_2} \right\rceil + 1, 4 \left\lceil \frac{|uv|}{\Delta_4} \right\rceil + 3 \right\}.$$

The expression of Δ can be derived through a comparison between Δ_1 , Δ_2 , and Δ_4 as follows (rounding and constants are ignored): 1) $\Delta = \frac{4}{\Delta_1}$, when the range ratio is between 2 and $\sqrt{5}$, 2) $\Delta = \frac{2}{\Delta_2}$, when the range ratio is between $\sqrt{5}$ and 3.8, and 3) $\Delta = \frac{1}{\Delta_4}$, when the range ratio is greater than 3.8. The asymptotic bound on network dilation under BVGF, $\tilde{D}_n(BVGF)$, can be computed by substituting the network length $\tau_G(u, v)$ by the expression of Δ in Definition 1. We have the following theorem:

Theorem 7. *The asymptotic network dilation of a sensing-covered network under BVGF satisfies*

$$\tilde{D}_n(BVGF) \leq \begin{cases} \frac{4R_c}{\sqrt{R_c^2 - R_s^2}} & (2 \leq R_c/R_s \leq \sqrt{5}) \\ \frac{2R_c}{\sqrt{R_c^2 - 4R_s^2}} & (\sqrt{5} < R_c/R_s \leq 3.8) \\ \frac{R_c}{\sqrt{R_c^2 - 2R_c R_s - R_s^2}} & (R_c/R_s > 3.8). \end{cases} \quad (5)$$

6.3 Summary of Analysis on Network Dilations

In this section, we summarize the network dilation bounds based on the deterministic communication model. Fig. 8a in Section 8 shows the DT-based dilation bound and the asymptotic dilation bounds of GF and BVGF under different range ratios. The asymptotic bound of BVGF is competitive for all range ratios no smaller than two. The bound gets the worst-case value $\frac{8\sqrt{3}}{3} \approx 4.62$ when $R_c/R_s = 2$. That is, BVGF can always find a routing path between any two nodes u and v within $4.62 \left\lceil \frac{|uv|}{R_c} \right\rceil$ hops. The asymptotic network dilation bound of GF increases quickly with the range ratio and approaches infinity when R_c/R_s is close to two. Whether there is a tighter bound for GF in such a case is an open research question. When $R_c/R_s \gg 3.5$, the network dilations of GF and BVGF are very similar because the network topology is dense and both algorithms can find

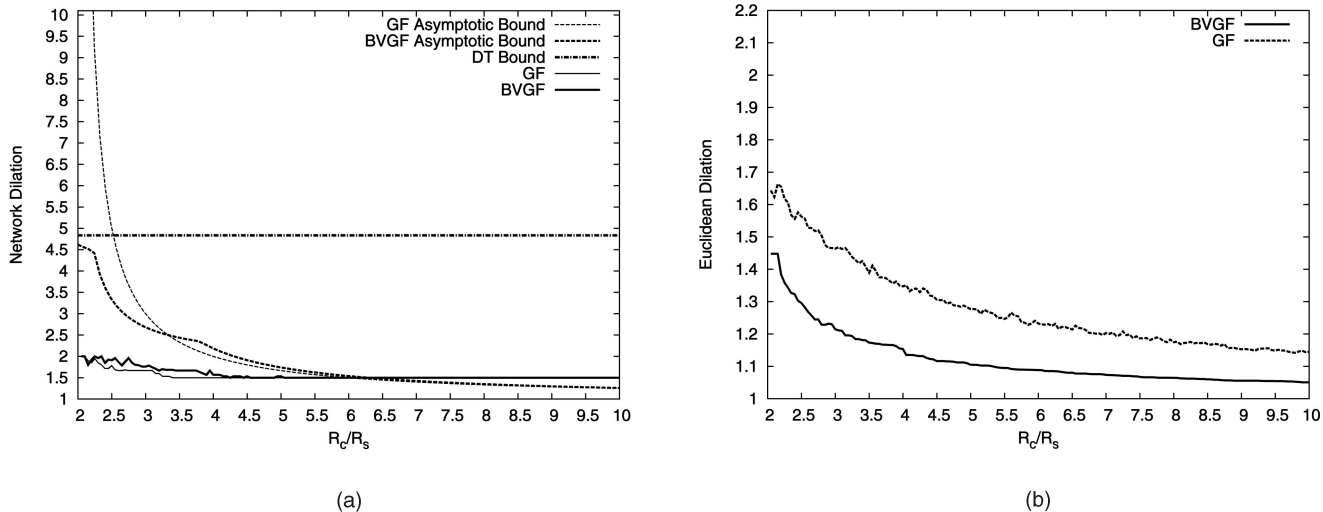


Fig. 8. Dilations based on the deterministic communication model. (a) Network dilation and (b) Euclidean dilation.

very short routing paths. The network dilation bound based on DT is significantly higher than the bounds of BVGF and GF when R_c/R_s becomes larger than ~ 2.5 because the analysis based on DT only considers DT edges (which is shown to be shorter than $2R_s$ in Lemma 2) and becomes conservative when the communication range is much larger than the sensing range.

7 EXTENSION BASED ON A PROBABILISTIC COMMUNICATION MODEL

The theoretical analysis and protocol design discussed in previous sections are based on a simplistic communication model that assumes a deterministic communication range. Recent empirical studies show that real sensor network platforms (e.g., Berkeley motes) yield unreliable links and irregular communication ranges [40]. A wireless sensor network must handle communication failures due to unreliable links. GF is shown to yield poor performance in lossy networks because it always chooses the node closest to the destination as the next hop, which often results in a long but unreliable communication link [26]. In this section, we extend our results to a probabilistic communication model that captures these characteristics.

In the probabilistic communication model, the quality of a communication link from node u to node v is described by *packet reception rate* ($PRR(u, v)$) that is defined as the ratio of the number of successful transmissions from u to v to the total number of transmissions from u to v . Note that $PRR(u, v)$ may not equal $PRR(v, u)$ since the communication quality of a link is often asymmetric. In practice, the PRR of a link can be estimated either offline or online. For example, in the MT routing protocol on TinyOS [35], a node computes the PRR of the link from a neighbor to itself by monitoring the reception statistics of periodic beacon messages broadcast by the neighbor.

7.1 Routing Algorithms with ARQ

When a node fails to deliver a packet to the next hop (e.g., indicated by a missing ACK from the receiver), it

retransmits the packet through an automatic repeat request (ARQ) mechanism. We assume ARQ keeps retransmitting a packet until successful reception by the next hop node. In this section, we discuss efficient variants of GF and BVGF when ARQ is employed. The case without ARQ is discussed in Section 7.2. Recently, Kuruville et al. studied several efficient routing metrics in presence of ARQ, including the product of PRR and progress traversed toward the destination, for wireless networks with a lossy physical layer [19]. Product of PRR and progress is also shown to be optimal in terms of energy efficiency for GF in [26] in lossy networks. This new metric achieves a better energy-efficiency than distance by balancing the hop count and path reliability. Both GF and BVGF can be modified to use this metric as follows: Instead of choosing the neighbor closest to destination among all routing candidates, node u chooses as the next hop a node v that maximizes $(|ut| - |vt|) \cdot PRR(u, v)$, where t is the destination. We denote the variants of GF and BVGF based on this new metric as GF_e and $BVGF_e$, respectively.

We extend the double range property presented in Section 3.2 as follows: For a given parameter p ($0 < p \leq 1$), we define the *probabilistic communication range* $R_c(p)$ as the distance within which the link of any two nodes has a PRR no lower than p . The extended double range property can be formulated as $R_c(p) \geq 2R_s$. Arguments similar to the proofs of Theorems 3 and 5 can show that both GF_e and $BVGF_e$ always find a routing path between any two nodes if $\exists p > 0$ s.t. $R_c(p) \geq 2R_s$. We note that the notation of $R_c(p)$ is only for the purpose of performance bound analysis. The operation of the GF_e and $BVGF_e$ does not require the knowledge of $R_c(p)$.

The analysis presented in Sections 4, 5, and 6 focuses on hop count and network dilation. However, in the probabilistic communication model, hop count does not indicate the quality of a routing path due to unreliable links. When ARQ is present, the energy cost and end-to-end delay of a routing path depends on the total number of transmissions needed to successfully deliver a packet from source to destination. Hence, the total number of transmissions is a more accurate metric to describe the quality of a routing path. Before extending the analytical results based on the number of

transmissions, we define the following notation: $\tilde{D}_n(GF)$ and $\tilde{D}_n(BVGF)$ represent the asymptotic network dilation bounds by replacing R_c with $R_c(p)$ in (4) and (5). For a given routing algorithm, Δ_i represents the progress toward the destination made at the i th step of the algorithm, p_i represents the PRR of the link chosen at the i th step, and Δ' represents the minimum progress toward the destination made by the algorithm if only considering the neighbors within $R_c(p)$. We have the following theorem regarding the performance of GF_e and $BVGF_e$.

Theorem 8. *In a sensing-covered network that satisfies the double range property for a probabilistic communication range $R_c(p)$, the asymptotic expected total number of transmissions used by algorithm A_e (A is GF or $BVGF$) to deliver a packet between two nodes u and v is no smaller than $\tilde{D}_n(A) \cdot |uv| / (p \cdot R_c(p))$ in the presence of ARQ.*

Proof. According to the definition of $R_c(p)$, the PRR of any link within $R_c(p)$ is no lower than p . Since A_e chooses the next-hop node that has the maximum product of progress and PRR, we have:

$$\forall i, \Delta_i \cdot p_i \geq \Delta' \cdot p. \quad (6)$$

For a link with PRR p_i , the expected number of transmissions is equal to $1/p_i$. From (6), the total number of transmissions between source s and destination t satisfies the following inequality:

$$\sum_i \frac{1}{p_i} \leq \frac{\sum_i \Delta_i}{\Delta' \cdot p} = \frac{|st|}{\Delta' \cdot p}. \quad (7)$$

According to the definition of network dilation, $\Delta' = R_c(p) / \tilde{D}_n(A)$. Replacing Δ' in (7) gives the form in the statement of the theorem. \square

Theorem 8 shows that both GF_e and $BVGF_e$ can find routing paths with a bounded number of transmissions in the presence of ARQ in lossy networks.

7.2 Routing Algorithms without ARQ

In this section, we discuss efficient variants of GF and $BVGF$ without the support of ARQ. When ARQ is not implemented, a node drops a packet if it fails to deliver it to the next-hop node. The quality of a routing path can be quantified by *end-to-end reliability* defined as the probability that a packet can be successfully transmitted from source to destination along the path. It can be seen that the end-to-end reliability of a routing path is equal to the product of the PRR of each link on the path. We propose a new metric $(|ut| - |vt|) / \ln \frac{1}{PRR(u,v)}$ (where u , v , and t are routing node, a neighbor of u and destination, respectively) that provides lower-bounded end-to-end reliability when used with GF and $BVGF$. We refer to GF and $BVGF$ based on this new metric as GF_r and $BVGF_r$, respectively. We have the following theorem regarding the performance of GF_r and $BVGF_r$:

Theorem 9. *In a sensing-covered network that satisfies the double range property for a probabilistic communication range $R_c(p)$, the asymptotic end-to-end reliability of the path found by*

algorithm A_r (A is GF or $BVGF$) is no lower than $e^{\tilde{D}_n(A) \cdot |uv| \cdot \ln p / R_c(p)}$.

Proof. Since A_r always chooses the next-hop node that has the maximum $\Delta_i / \ln \frac{1}{p_i}$, we have:

$$\forall i, \frac{\Delta_i}{\ln 1/p_i} \geq \frac{\Delta'}{\ln 1/p}. \quad (8)$$

From (8), we have the following inequality:

$$\sum_i \ln p_i \geq \frac{\sum_i \Delta_i \cdot \ln p}{\Delta'} = \frac{|st| \cdot \ln p}{\Delta'}. \quad (9)$$

From (9), the reliability of a routing path found by A_r between source s and destination t satisfies $\prod_i p_i \geq e^{\frac{|st| \cdot \ln p}{\Delta'}}$. Replacing Δ' with $R_c(p) / \tilde{D}_n(A)$ (by the definition of $\tilde{D}_n(A)$) gives the form in the statement of the theorem. \square

Theorem 9 shows that both GF_r and $BVGF_r$ can find routing paths with bounded end-to-end reliability in absence of ARQ.

8 SIMULATION RESULTS

In this section, we present our simulation results. The purpose of the simulations is twofold. First, we compare the dilations of GF and $BVGF$ under different range ratios and investigate the tightness of the dilation bounds we derived in previous sections. We then study the average performance of the algorithms under a realistic radio model of the Mica2 motes [8].

8.1 Results Based on the Deterministic Communication Model

Our first set of simulations are based on the deterministic communication model. 1,000 nodes are randomly distributed in a $500m \times 500m$ region that is covered by a set of active nodes chosen by the Coverage Configuration Protocol (CCP) [33]. Redundant nodes are turned off for energy conservation. All nodes have the same sensing range of $20m$. We vary R_c to measure the network and Euclidean dilations of GF and $BVGF$ under different range ratios. As discussed in Section 5, the routing metric of GF is based on Euclidean or projected distance. Since the results of the two metrics are very similar, only Euclidean-distance-based results are presented in this section.

The results presented in this section are averages of five runs on different network topologies produced by CCP. In each round, a packet is sent from each node to every other node in the network. As expected, all packets are delivered by both algorithms. The network and Euclidean lengths are logged and the dilations are then computed using Definitions 1 and 2, respectively. To distinguish the simulation results from the dilation bounds we derived in previous sections, we refer to the former as *measured dilations*. We should note that the measured dilations characterize the average-case performance of the routing algorithms in the particular network topologies used in our experiments, which may differ from the worst-case bounds for *all* possible sensing-covered network topologies we derived in previous sections.

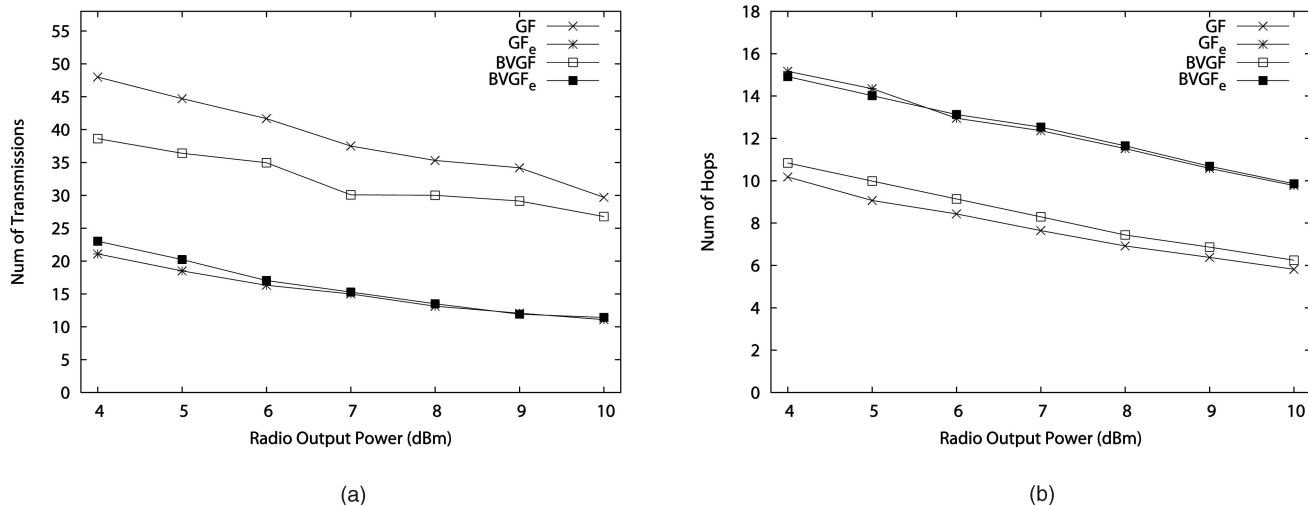


Fig. 9. Performance with ARQ based on the probabilistic communication model. (a) Average total number of transmissions per path. (b) Average hop count per path.

Fig. 8a shows that the measured dilations of GF and BVGF remain close to each other. Both algorithms have very low dilations (smaller than two) in all range ratios no smaller than two. When R_c/R_s increases, the measured dilations of both algorithms approach their asymptotic bounds. When R_c/R_s is close to 2, however, the difference between the asymptotic bounds and the corresponding measurements becomes wider. This is because the worst-case scenarios from which the dilation bounds are derived are rare when the network is less dense. Due to the rounding errors in deriving the asymptotic dilation bounds (Corollary 2 and Theorem 7), the measured dilations are slightly higher than the asymptotic bounds when $R_c/R_s > 6$, as shown in Fig. 8a. This is because, when R_c becomes large, the routing paths become very short and the effect of rounding in the calculation of network dilations becomes significant. The result also indicates that the measured dilation of GF is significantly lower than the asymptotic bound derived in this paper. Whether or not GF has a tighter network dilation bound is left for our future work. Fig. 8b shows the Euclidean dilations of GF and BVGF. BVGF outperforms GF for all range ratios. This is due to the fact that BVGF always forwards a packet inside the Voronoi forwarding rectangle. As mentioned in Section 3, the low Euclidean dilation may lead to potential energy savings in wireless communications.

The simulation results have shown that the proposed BVGF algorithm performs similarly with GF in average cases and has lower Euclidean dilation. In addition, the upper bounds on the network dilations of BVGF and GF established in previous sections are tight when R_c/R_s is large.

8.2 Results Based on the Probabilistic Communication Model

In this section, we evaluate the performance of the extended versions of GF and BVGF algorithms discussed in Section 7 in lossy networks. To simulate the probabilistic link reception quality, we implemented the link layer model from USC [41]. Previous empirical data shows that the USC model accurately simulates the unreliable links between

Mica2 nodes [41]. In our simulations, the PRR of a link is governed by the USC model according to the distance between the two nodes and the transmission power. A packet is sent using different routing algorithms between any two nodes that are more than 350m apart. A node ignores the neighbors whose links have a PRR lower than 10 percent. Previous study [35] showed that such “black-listing” strategy can significantly improve the packet delivery performance. The rest of simulation settings are the same as those in Section 8.1.

We first evaluate the performance of our algorithms with ARQ. Fig. 9a and Fig. 9b show the average number of transmissions and hops under different radio transmission powers set according to the specification of Mica2 mote [8]. The minimum power is chosen such that all neighbors within $2R_s$ of a node have PRRs above 10 percent and, thus, are not blacklisted. Consistent with our analysis, this condition made all algorithms successfully deliver all packets. Fig. 9a shows that all algorithms yielded fewer transmissions when the transmission power increases. GF_e and BVGF_e perform substantially better than GF and BVGF, although GF and BVGF used fewer hops shown by Fig. 9b. This result confirms the observation that product of progress and PRR is an efficient metric for greedy forwarding in lossy networks [26]. BVGF_e yielded similar performance as GF_e, which is consistent with the results based on the deterministic communication model.

We now evaluate the performance of our algorithms without ARQ. Fig. 10a and Fig. 10b show the average end-to-end reliability and hop counts of different algorithms. We can see that both GF and BVGF yielded near zero end-to-end path reliability, although they used fewer hops. This is because they tend to choose long links which, however, are more likely to be unreliable. In contrast, both GF_r and BVGF_r achieved higher end-to-end reliability as transmission power increases since the PRR of the link at each hop becomes higher. Although GF_r used more hops than BVGF_r, as shown in Fig. 10b, GF_r performs slightly better than BVGF_r, as it has more next hop candidates and, hence, a higher chance of choosing more reliable links.

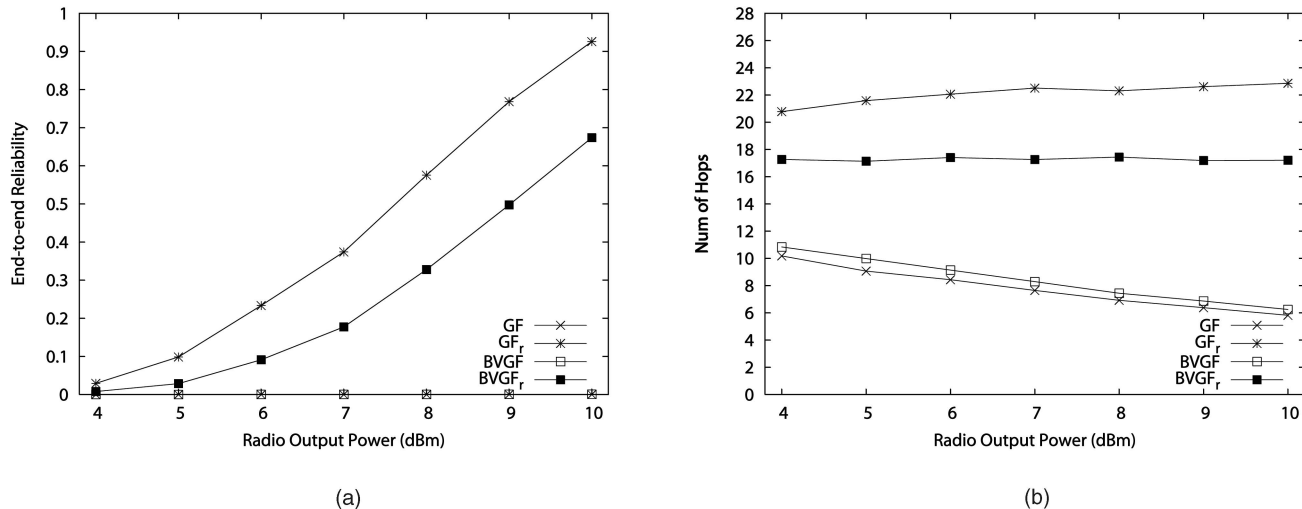


Fig. 10. Performance without ARQ based on the probabilistic communication model. (a) Average end-to-end reliability per path. (b) Average hop count per path.

The overall results in this section show that the routing metrics that consider both progress and PRR are more efficient than a purely progress-based metric in lossy networks. The extended GF and BVGF based on these metrics can achieve satisfactory performance in terms of number of transmissions and reliability on sensing-covered networks with unreliable communication links.

9 CONCLUSION

Our results lead to several important insights into the design of sensor networks. First, our analysis and simulation show that simple greedy geographic routing algorithms such as GF and BVGF may be highly efficient in sensing-covered networks with deterministic or probabilistic communication links. Second, our results indicate that the redundant nodes can be turned off without a significant increase in network length as long as the remaining active nodes maintain sensing coverage. Therefore, our analysis justifies coverage maintenance protocols [31], [33], [37], [38] that conserve energy by scheduling nodes to sleep. Finally, our dilation bounds enable a source node to efficiently compute an upper-bound on the network length or expected number of transmissions of its routing path based on the location of the destination. This capability can be useful to real-time communication protocols that require such bounds to achieve predictable end-to-end communication delays.

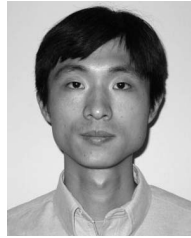
ACKNOWLEDGMENTS

This work was supported in part by the US National Science Foundation under an ITR grant CCR-0325529.

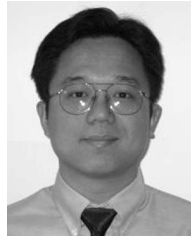
REFERENCES

- [1] F. Aurenhammer, "Voronoi Diagrams—A Survey of a Fundamental Geometric Data Structure," *ACM Computing Surveys*, vol. 23, no. 3, pp. 345-405, 1991.
- [2] F. Baccelli, K. Tchoumatchenko, and S. Zuyev, "Markov Paths on the Poisson-Delaunay Graph with Applications to Routing in Mobile Networks," *Advances Applied Probability*, vol. 32, 2000.
- [3] P. Bose and P. Morin, "Online Routing in Triangulations," *ISAAC: Proc. 10th Int'l Symp. Algorithms and Computation*, 1999.
- [4] P. Bose, P. Morin, I. Stojmenovic, and J. Urrutia, "Routing with Guaranteed Delivery in Ad Hoc Wireless Networks," *Wireless Networks*, vol. 7, no. 6, pp. 609-616, 2001.
- [5] K. Chakrabarty, S.S. Iyengar, H. Qi, and E. Cho, "Grid Coverage for Surveillance and Target Location in Distributed Sensor Networks," *IEEE Trans. Computers*, vol. 51, no. 12, pp. 1448-1453, Dec. 2002.
- [6] L. Chew, "There Is a Planar Graph Almost as Good as the Complete Graph," *Proc. Second Ann. ACM Symp. Computational Geometry*, pp. 169-177, 1986.
- [7] T. Couqueur, V. Phipatanasuphorn, P. Ramanathan, and K.K. Saluja, "Sensor Deployment Strategy for Target Detection," *Proc. First ACM Int'l Workshop Wireless Sensor Networks and Applications*, pp. 169-177, Sept. 2002.
- [8] Crossbow, Mica, and Mica2 Wireless Measurement System Datasheets, 2003.
- [9] D.P. Dobkin, S.J. Friedman, and K.J. Supowit, "Delaunay Graphs Are Almost as Good as Complete Graphs," *Discrete and Computational Geometry*, 1990.
- [10] M. Duarte and Y.-H. Hu, "Distance Based Decision Fusion in a Distributed Wireless Sensor Network," *Proc. Second Int'l Workshop Information Processing in Sensor Networks (IPSN 2003)*, Apr. 2003.
- [11] D. Eppstein, "Spanning Trees and Spanners," Technical Report ICS-TR-96-16, 1996.
- [12] G. Finn, "Routing and Addressing Problems in Large Metropolitan-Scale Internetworks," Technical Report ISI Research Report ISU/RR-87-180, Inst. for Scientific Information, Mar. 1987.
- [13] J. Gao, L.J. Guibas, J. Hershberger, L. Zhang, and A. Zhu, "Geometric Spanner for Routing in Mobile Networks," *Proc. Second ACM Symp. Mobile Ad Hoc Networking and Computing (MobiHoc '01)*, pp. 45-55, Oct. 2001.
- [14] G.L. Goodman, "Detection and Classification for Unattended Ground Sensors," *Proc. Information Decision and Control '99*, pp. 419-424, Feb. 1999.
- [15] J.M. Keil and C.A. Gutwin, "Classes of Graphs Which Approximate the Complete Euclidean Graph," *Discrete Computational Geometry*, no. 7, 1992.
- [16] B. Karp and H.T. Kung, "GPSR: Greedy Perimeter Stateless Routing for Wireless Networks," *Proc. Sixth ACM Int'l Conf. Mobile Computing and Networking (MobiCom '00)*, pp. 243-254, 2000.
- [17] E. Kranakis, H. Singh, and J. Urrutia, "Compass Routing on Geometric Networks," *Proc. 11th Canadian Conf. Computational Geometry*, pp. 51-54, Aug. 1999.
- [18] F. Kuhn, R. Wattenhofer, and A. Zollinger, "Worst-Case Optimal and Average-Case Efficient Geometric Ad-Hoc Routing," *Proc. Fourth ACM Int'l Symp. Mobile Ad-Hoc Networking and Computing (MobiHoc)*, 2003.
- [19] J. Kuruvila, A. Nayak, and I. Stojmenovic, "Hop Count Optimal Position Based Packet Routing Algorithms for Ad Hoc Wireless Networks with a Realistic Physical Layer," *Proc. First IEEE Int'l Conf. Mobile Ad-Hoc and Sensor Systems (MASS)*, 2004.

- [20] D. Li, K. Wong, Y.H. Hu, and A. Sayeed, "Detection, Classification and Tracking of Targets in Distributed Sensor Networks," *IEEE Signal Processing Magazine*, vol. 19, no. 2, Mar. 2002.
- [21] J. Li, J. Jannotti, D.S.J. D. Couto, D.R. Karger, and R. Morris, "A Scalable Location Service for Geographic Ad-Hoc Routing," *Proc. Sixth ACM Int'l Conf. Mobile Computing and Networking (MobiCom '00)*, pp. 120-130, Aug. 2000.
- [22] X.-Y. Li, G. Calinescu, and P.-J. Wan, "Distributed Construction of a Planar Spanner and Routing for Ad Hoc Wireless Networks," June 2002.
- [23] M. Mauve, J. Widmer, and H. Hartenstein, "A Survey on Position-Based Routing in Mobile Ad Hoc Networks," 2001.
- [24] S. Meguerdichian, F. Koushanfar, M. Potkonjak, and M.B. Srivastava, "Coverage Problems in Wireless Ad-Hoc Sensor Networks," *Proc. INFOCOM*, pp. 1380-1387, 2001.
- [25] R. Ramanathan and R. Hain, "Topology Control of Multihop Wireless Networks Using Transmit Power Adjustment," *Proc. INFOCOM*, 2000.
- [26] K. Seada, M. Zuniga, A. Helmy, and B. Krishnamachari, "Energy-Efficient Forwarding Strategies for Geographic Routing in Lossy Wireless Sensor Networks," *Proc. Second Int'l Conf. Embedded Networked Sensor Systems (SenSys '04)*, 2004.
- [27] Sensoria, "SGate Datasheet," 2003.
- [28] SonicWall, "Long Range Wireless Card Datasheet," 2003.
- [29] I. Stojmenovic and X. Lin, "Loop-Free Hybrid Single-Path/Flooding Routing Algorithms with Guaranteed Delivery for Wireless Networks," *IEEE Trans. Parallel and Distributed Systems*, vol. 12, no. 10, pp. 1023-1032, Oct. 2001.
- [30] H. Takagi and L. Kleinrock, "Optimal Transmission Ranges for Randomly Distributed Packet Radio Terminals," *IEEE Trans. Comm.*, vol. 32, no. 3, pp. 246-257, 1984.
- [31] D. Tian and N.D. Georganas, "A Coverage-Preserved Node Scheduling Scheme for Large Wireless Sensor Networks," *Proc. First Int'l Workshop Wireless Sensor Networks and Applications (WSNA '02)*, pp. 169-177, Sept. 2002.
- [32] P. Varshney, *Distributed Detection and Data Fusion*. New York: Springer-Verlag, 1996.
- [33] G. Xing, X. Wang, Y. Zhang, C. Lu, R. Pless, and C.D. Gill, "Integrated Coverage and Connectivity Configuration for Energy Conservation in Sensor Networks," *ACM Trans. Sensor Networks*, vol. 1, no. 1, 2005.
- [34] R. Wattenhofer, L. Li, P. Bahl, and Y.-M. Wang, "Distributed Topology Control for Wireless Multihop Ad-Hoc Networks," *Proc. INFOCOM*, pp. 1388-1397, 2001.
- [35] A. Woo, T. Tong, and D. Culler, "Taming the Underlying Challenges of Reliable Multihop Routing in Sensor Networks," *SenSys*, 2003.
- [36] G. Xing, C. Lu, R. Pless, and Q. Huang, "On Greedy Geographic Routing Algorithms in Sensing-Covered Networks," *Proc. Fifth ACM Symp. Mobile Ad Hoc Networking and Computing (MobiHoc '04)*, May 2004.
- [37] T. Yan, T. He, and J.A. Stankovic, "Differentiated Surveillance for Sensor Networks," *Proc. First Int'l Conf. Embedded Networked Sensor Systems (SenSys '03)*, 2003.
- [38] F. Ye, G. Zhong, S. Lu, and L. Zhang, "PEAS: A Robust Energy Conserving Protocol for Long-Lived Sensor Networks," *Proc. 23rd Int'l Conf. Distributed Computing Systems (ICDCS '03)*, pp. 169-177, May 2003.
- [39] H. Zhang and J.C. Hou, "Maintaining Coverage and Connectivity in Large Sensor Networks," *The Wireless Ad Hoc and Sensor Networks: An Int'l J.*, 2005.
- [40] J. Zhao and R. Govindan, "Understanding Packet Delivery Performance in Dense Wireless Sensor Networks," *Sensys*, Nov. 2003.
- [41] M. Zuniga and B. Krishnamachari, "Analyzing the Transitional Region in Low Power Wireless Links," *Proc. First IEEE Int'l Conf. Sensor and Ad Hoc Comm. and Networks (SECON)*, Oct. 2004.



Guoliang Xing received the BS degree in electrical engineering in 1998 and the MS degree in computer science in 2001, both from Xi'an Jiaotong University, Xi'an, China. He is currently a PhD candidate in the Department of Computer Science and Engineering at Washington University in St. Louis. His research interests include power management in wireless sensor networks, spatiotemporal data services in wireless sensor networks, and middleware for networked embedded systems. He is a student member of the IEEE.



Chenyang Lu received the PhD degree from the University of Virginia in 2001, the MS degree from the Chinese Academy of Sciences in 1997, and the BS degree from the University of Science and Technology of China in 1995, all in computer science. He is an assistant professor in the Department of Computer Science and Engineering at Washington University in St. Louis. His current research interests include wireless sensor networks, real-time and embedded systems and middleware, and adaptive QoS control. He is author and coauthor of more than 40 refereed papers. He received the US National Science Foundation CAREER Award in 2005. He is a member of the IEEE and the IEEE Computer Society.



Robert Pless received the BS degree in computer science in 1994 from Cornell University and the PhD degree in computer science from the University of Maryland in 2000. He is currently an assistant professor of computer science and the assistant director of the Center for Security Technologies at Washington University in St. Louis. His field of research is computer vision, with a concentration in extreme camera geometries, panoramic vision, sensor fusion, and manifold learning, and he served as chairman of the 2003 IEEE International Workshop on Omni-Directional Vision and Camera Networks (Omnivis '03). He is a member of the IEEE and the IEEE Computer Society.



Qingfeng Huang received the DSc degree in computer science from Washington University in St. Louis in August 2003, the AM degree in physics from Washington University in August 1998, and the BS degree in physics from Fudan University in 1992. He has published papers in multiple areas, including mobile computing, sensor networks, intelligent transportation systems, neuroscience, and quantum physics. His current research interests include algorithms and middleware for ubiquitous computing, sensor networks, and artificial intelligence. He is currently a research scientist at the Palo Alto Research Center (PARC) and a member of the IEEE and the IEEE Computer Society.

► For more information on this or any other computing topic, please visit our Digital Library at www.computer.org/publications/dlib.